

Construction of Stable Superhydrophobic Al Surface with Improved Corrosion Resistance

Mei Ji

Department of Electronics and Communication Engineering, Suzhou Institute of Industrial Technology, Suzhou 215104, China.

iceyair11@163.com

Abstract

We presented a simple anodic oxidation process and post-modification for construction of superhydrophobic Al surface with improved corrosion resistance. The Al sheets were first anodized in H_3PO_4 aqueous solution and were then modified with stearic acid (SA) in solvent to lower the surface energy. The sample surface morphologies, chemical compositions, bonding states, wettability and corrosion resistance were investigated by scanning electron microscopy (SEM), Atomic force microscopy (AFM), contact angle (CA) measurements, and electrochemical measurements.

Keywords

Superhydrophobic Al surfaces; Corrosion resistance; Surface energy.

1. Introduction

We presented a simple anodic oxidation process and post-modification for construction of superhydrophobic Al surface with improved corrosion resistance. The Al sheets were first anodized in H_3PO_4 aqueous solution and were then modified with stearic acid (SA) in solvent to lower the surface energy. The sample surface morphologies, chemical compositions, bonding states, wettability and corrosion resistance were investigated by scanning electron microscopy (SEM), Atomic force microscopy (AFM), contact angle (CA) measurements, and electrochemical measurements.

The corrosion of metals and metal-based materials in the humid atmosphere or aqueous environment restricts their further applications and results in serious environmental contamination and huge waste. Al and its alloys, an important class of engineering materials, although protected by a thin and compact oxide film, are susceptible to corrosion in aggressively corrosive environment. In order to extend their practical applicabilities, corrosion-resistant anodized layers, zeolites, and chromate-based coatings are frequently utilized to protect the underlying Al substrates from corrosion [1-4]. Nevertheless, these preparations are subject to special equipments or techniques, severe processing conditions, and even toxic, strictly regulated. Therefore, it is imperative to introduce a sufficient corrosion protection strategy maximizing the utility of Al and its alloys through a simple, facile, and chromium-free method.

Since the first superhydrophobic surface was observed on lotus leaf in 1997, researchers and engineers have been inspiring by the superhydrophobicity for its importance in fundamental research as well as potential applications including anti-freezing, aquatic walking devices, oil/water separation, friction reduction, and water collection, *etc* [5-9]. Mostly motivated by the desire to take advantage of the intrinsic water-proof characteristics of superhydrophobic surfaces, human beings have developed numerous metallic surfaces with special wettability providing enhanced corrosion resistance of the underlying metal substrates [10-14]. As such, the migration of the aggressive ions such as chloridion can be prevented by the "air valleys" in which the large amount of air is trapped within the valleys between the hierarchically textured structures of superhydrophobic surfaces. In this way, a ZnAl-LDH (Layered double hydroxides)-laurate superhydrophobic film was constructed by anion exchange on aluminum substrate, which provided long-term corrosion protection of the coated aluminum substrate from corrosion [15]. Liang *et al.* successfully fabricated a fluoroalkylsilane (FAS:

$\text{CH}_3(\text{CF}_2)_6(\text{CH}_2)_3\text{Si}(\text{OCH}_3)_3$ modified hydroxide zinc carbonate superhydrophobic Al surface to enhance its corrosion resistance in corrosive medium [16]. Recently, our group reported that long-chain fatty acids modified Al surfaces displaying stable superhydrophobic property and delayed-icing effects [17,18]. However, the corrosion resistance of the superhydrophobic Al surface has not yet investigated.

Herein, we present a simple method for fabrication of superhydrophobic Al surfaces with improved corrosion resistance. The Al sheets were first chemically etched in HCl aqueous solution and then modified with SA to lower the surface energy in DMF/water mixture solvent with different ratio of DMF to water. The water repellent property and corrosion resistance of the as-prepared Al surfaces were increasingly improved with the increase of the ratio of DMF to water.

2. Experimental Procedures

2.1 Pretreatment of Al

Industrial aluminum sheets (Al 99.99) were cut into 40 mm × 60 mm rectangular strips with a thickness of 0.5 mm and then cleaned ultrasonically with acetone and deionized water for 5 min, respectively. The cleaned samples were then immersed in 1 M NaOH aqueous solution for 1 min at room temperature. After the immersion, the samples were rinsed with deionized water and dried in air at room temperature.

2.2 Preparation of Superhydrophobic Al Surface

The pretreated Al substrates were chemically etched in 2.6 M HCl aqueous solution at room temperature for 1.5 min and were thoroughly rinsed with deionized water. The Al substrate was then modified with SA in a DMF/water mixture solvent containing 0.01 M SA at 99°C for 0.5 h. The ratio of DMF to water was changed from 0:1 (pure water), 1:1, 3:1, 6:1, 9:1, to 1:0 (pure DMF). The substrates were subsequently rinsed with absolute ethanol, and dried at room temperature for further characterization.

2.3 Characterization

The scanning electron microscopy (SEM) and energy dispersive X-ray spectroscopy (EDS) were carried out on a Sirion FEI instrument. X-ray photoelectron spectroscopy (XPS) measurements were performed on PHI 5000 Versa Probe, with a monochromatic Al K α X-ray source, and the spectra were referenced to the adventitious C 1s peak (284.6 eV). Atomic force microscopy (AFM) imaging was obtained by using the Veeco Dimension ICON system operating in tapping mode under ambient conditions. The sessile drop method was used for water CA measurements using a Dataphysics OCA15Pro contact-angle system at ambient temperature. Water droplet (3 μL) was dropped carefully onto the surface. The average CA value was determined by measuring 5 times at different spots of the same sample. The RA was measured under the same temperature and humidity as the CA measurements, and the volume of the droplet was 5 μL . The electrochemical measurements were operated in a conventional three-electrode electrochemical cell consisted of Mg alloy electrode as working electrode, a platinum as counter electrode and a standard calomel reference electrode (SCE) as the reference electrode by using a CHI 760 D electrochemical analyzer (CH Instruments, Shanghai Chenhua Co., China). The electrolyte is 3.5% NaCl aqueous solution. All measured potentials presented in this paper were referred to SCE. Tafel polarization curves were obtained by changing the electrode potential automatically with the sweep rate of 0.01 V s⁻¹.

3. Results and Discussion

Figure 1a is SEM image of the as-received Al surface showing that the surface was relatively smooth with many grinding and polishing lines. After immersion in NaOH aqueous solution, the surfaces became roughened with corpuscule-like structure (Figure 1b). The goal of the immersion is to remove the oxides on Al surfaces facilitating the following HCl-etching process. HCl-etched Al surfaces modified with SA display the typical porous morphology with many microscale cavities and

islands dispersed across surface (Figure 1c). A further observation (Figure 1c inset) shows nanoscale rectangle topography on the cavities and islands, the width of rectangle is about 200-400 nm, and the length is approximately 350-650 nm. Figure 1d is the cross-section SEM image of resultant superhydrophobic Al surface embedded in Bakelite, demonstrating that the thickness of the film is 290-320 nm. The HCl-etched Al surfaces with hierarchically micronanoscaled structures were obtained which can increase the surface roughness for the final construction of superhydrophobicity [5-9]. The composition of Al surfaces chemically etched by HCl and post-modified with SA was examined by EDS and the results were shown in Figure 1e inset. The EDS spectra clearly exhibited that C, O, Al components were detected, which indicated that Al surface had modified with SA. The wetting property of the samples was investigated by CA measurements. Al substrate was hydrophilic with a native oxidized layer having a CA of 85.9° (Figure 1a inset). After the Al samples were HCl-etched and subsequently modified with SA in the DMF/water mixture solvent with different ratio of DMF to water ranging from 0:1 (pure water), 1:1, 3:1, 6:1, 9:1, to 1:0 (pure DMF), the CAs on the resultant Al surfaces gradually increased from 121.6° , 143.0° , 148.8° , 154.2° , 163.4° , to 167.3° ; while the RAs decreased from 32.3° , 21.9° , 16.5° , 9.8° , 2.3° , to 1.5° (Figure 1f).

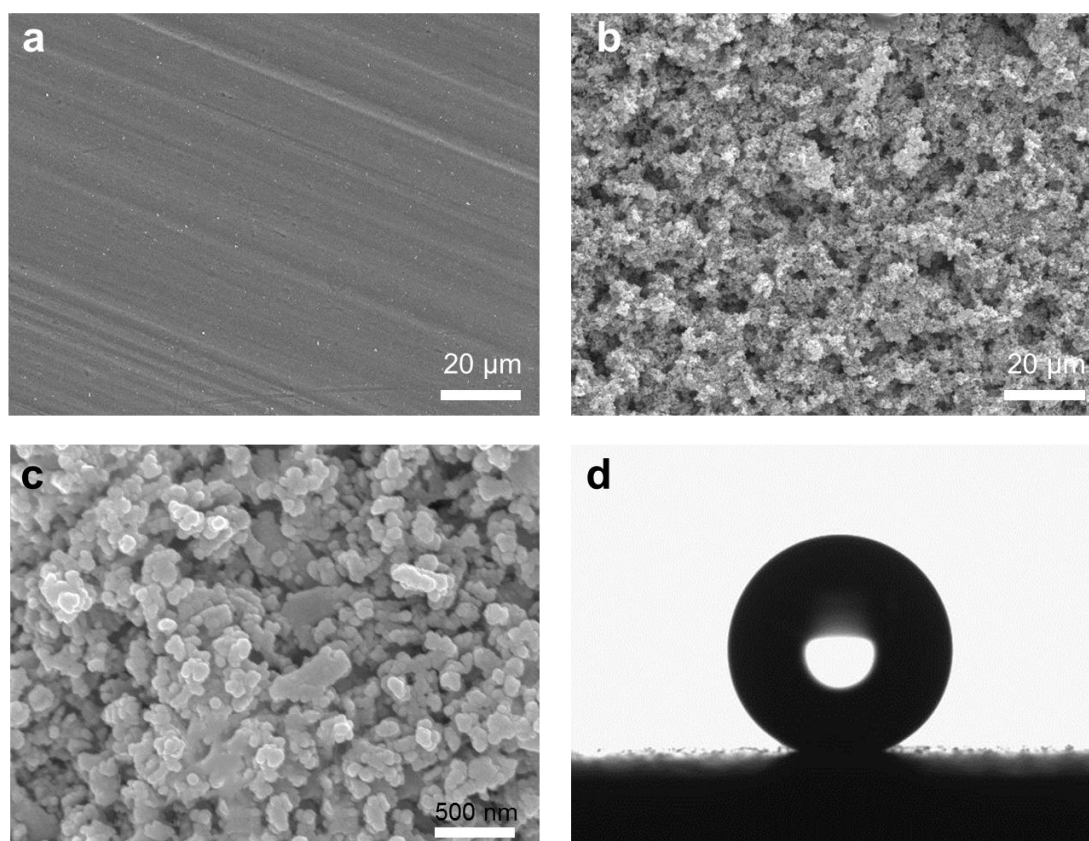


Figure 1: SEM image of the bare Al (a). SEM images of AAO-Al surface, the inset is higher magnification (b). The higher magnification of b showing hierarchically roughened structures (c).

Optical image of a water droplet with a contact angle of $163.6 \pm 2.7^\circ$ (d).

In general, the combination of low surface free energy and surface roughness contribute to the superhydrophobicity of the surface. And the Cassie-Baxter model is proposed to be responsible for the non-sticking superhydrophobic surface according to the fact that a rough hydrophobic surface can be considered as a hierarchical medium where the penetration of the liquid is not favorable [19,20]. On the other hand, according to Cassie-Baxter equation [20], $(\cos \theta^* = f(\cos \theta + 1) - 1)$, θ^* and θ are the CAs on the rough and flat surface, Here, θ is 98.0° , the CA on SA-modified flat Al surface. And

f is the fraction of solid/water interface per unit area, accordingly, $1-f$ is the fraction of air/water interface per unit area), the increasing fraction of air/water interface per unit area ($1-f$) should increase the CA on rough surface. So, when the Al HCl-etched samples were modified with SA in the DMF/water mixture with the ratio of DMF to water (0:1), ($1-f$) was 0.674, which means that air occupied 67.4% of the contact area between the water and the rough surface. In this way, as the ratio of DMF to water ranging from 1:1, 3:1, 6:1, 9:1, to 1:0, ($1-f$) was changed from 76.6%, 82.2%, 88.4%, 95.2%, to 97.2%. Thus, the combination of low surface free energy SA and hierarchical surface roughness as well as solvent effect is proposed to be responsible for these phenomena that water repellent of Al sheets were improved with the increase ratio of DMF to water.

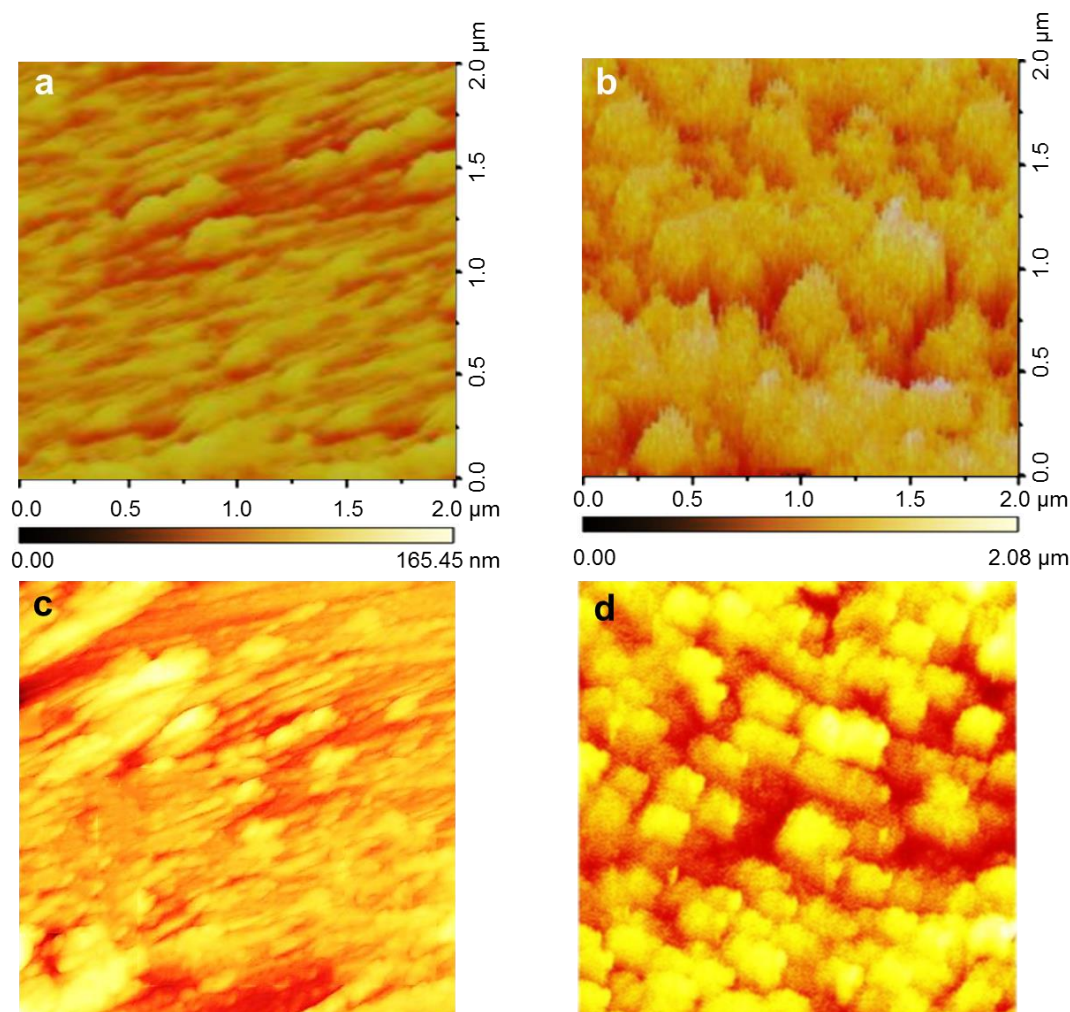


Figure 2: AFM images and corresponding cross-sectional roughness profiles of as-received Al surface (a), and superhydrophobic Al surface (b).

The morphology and roughness of as-received and superhydrophobic Al surface were also investigated by AFM. The 3D image and cross-sectional profile of the bare Al surface (Figure 3a) revealed a relatively planar morphology on numerous grinding and polishing lines. The rms (root-mean-square) roughness and the roughness factor which is the ratio of true solid surface area to its projected area demonstrated in Figure 3a are 30.3 nm and 1.05, respectively. As shown in Figure 3b, the superhydrophobic Al surface is composed of many cavities and islands. The rms and the roughness factor are found to be 855 nm and 6.89, respectively, which are greater than those of the as-received one. These results agree well with that of SEM.

The composition and binding states of Al surface after SA modification were also examined by XPS and the obtained results were presented in Figure 3. The XPS survey spectra (Figure 4a) demonstrated the elemental existence of C and O on the superhydrophobic Al surface. The deconvolution spectra for oxygen, aluminium, and carbon were shown in Figure 4b-d, respectively. The O 1s peak was observed at 531.2 eV. The peaks at 72.6 eV and 74.7 eV for Al 2p can be assigned to the elemental Al and Al (III) formed during the binding of SA at the Al substrate [21]. The C 1s peaks of 284.6 eV and 288.4 eV were attributed to aliphatic chain C-C, and carboxylate moiety COO⁻ involved in aluminum stearate, respectively, owing to two different carbon environments in SA [17,22,23]. This can further confirm the results of EDS analysis that SA has chemically adsorbed on the Al surface.

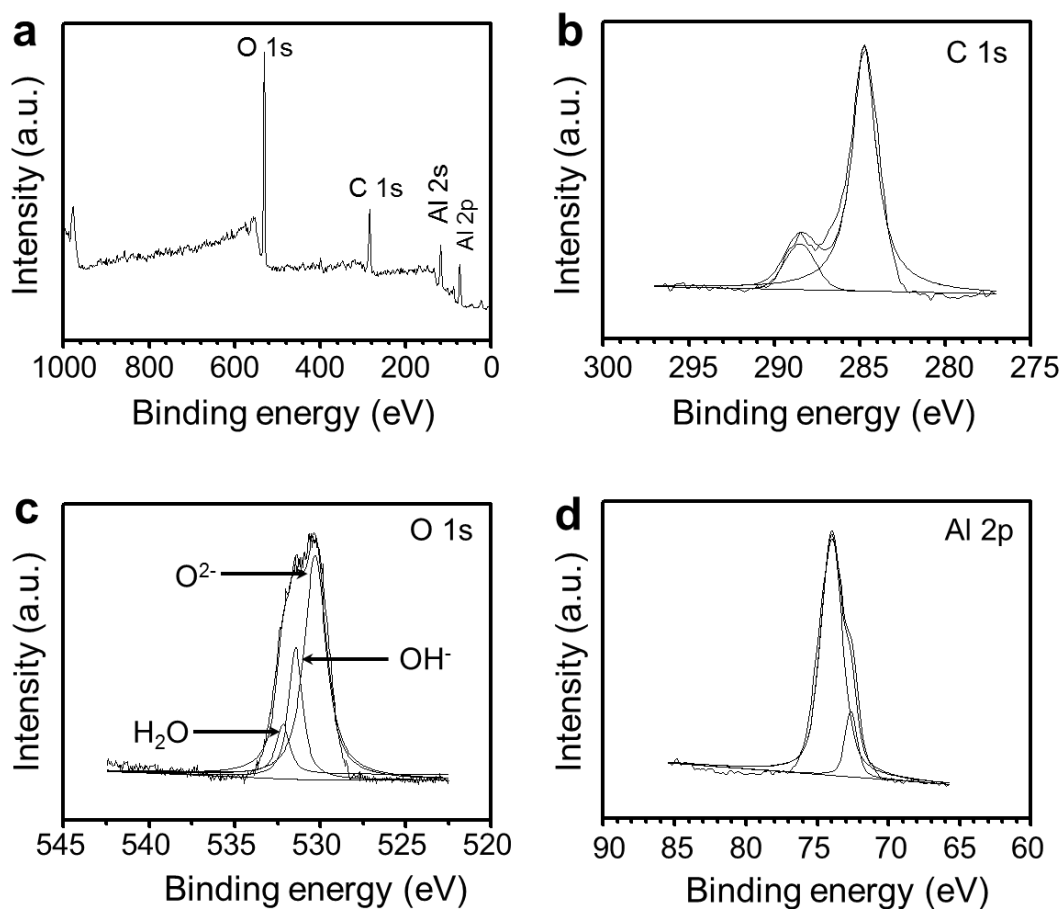


Figure 3: XPS survey spectra of superhydrophobic Al surface (a), and high-resolution XPS spectra in C 1s (b), O 1s (c), and Al 2p (d) spectral regions.

In order to investigate the corrosion properties of the bare Al and SA modified Al, Tafel polarization tests were performed in 3.5% NaCl aqueous solution. As shown in Figure 4A (a), the corrosion potential (E_{corr}) of the bare Al was -0.53 V vs.SCE and the corrosion current density (i_{corr}) was 3.24×10^{-4} A cm⁻². As such, the pitting corrosion occurred with hydrogen evolution in case that the Al samples were immersed in the aggressive corrosion environment with the presence of Cl⁻. After the Al samples were modified with SA in the DMF/water mixture solvent with different ratio of DMF to water ranging from 0:1, 1:1, 3:1, 6:1, 9:1 to 1:0, the E_{corr} of the SA modified Al samples shifted toward positive direction with the increase of the ratio of DMF to water in DMF/water mixture solvent (Figure 4A (b-e)), which indicated that the improvement of the protective properties of the SA modified Al surfaces generated significant alterations in the corrosion behavior and thus had the

potential to inhibit the corrosion of the Al substrates. Simultaneously, the i_{corr} of the SA modified Al samples decreased from $2.18 \times 10^{-4} \text{ A cm}^{-2}$, $1.86 \times 10^{-4} \text{ A cm}^{-2}$, $8.67 \times 10^{-6} \text{ A cm}^{-2}$, $1.59 \times 10^{-6} \text{ A cm}^{-2}$, $5.13 \times 10^{-7} \text{ A cm}^{-2}$, to $1.32 \times 10^{-7} \text{ A cm}^{-2}$ less than that of the as-received one. The detailed electrochemical measurement results were shown in Figure 4b. These results demonstrated that superhydrophobic surfaces largely improved the anticorrosion properties of the Al substrates.

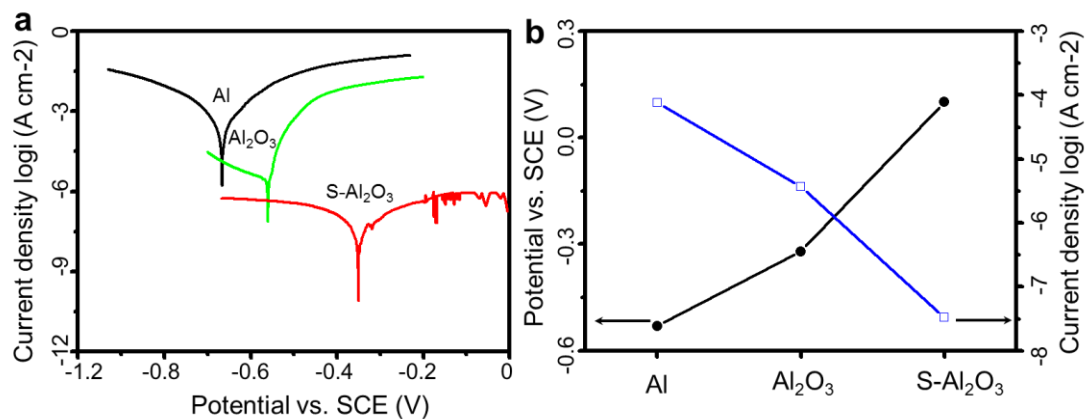


Figure 4: Tafel polarization curves obtained in 3.5% NaCl aqueous solution (a) and potentials and current densities panel (b) of as-received Al, Al₂O₃-Al, and superhydrophobic Al.

Also, we found that, in the Tafel polarization curve tests, the superhydrophobic Al surfaces were uneasily immersed in 3.5% NaCl aqueous solution compared to the as-prepared one; and the as-prepared Al substrates were immediately wetting when immersed in 3.5% NaCl. Thus, we considered that the corrosion rates of the samples were affected by the surface chemical compositions as well as the interfacial conditions. As shown in Figure 5, the as-received Al substrate contact with the corrosive media directly, and the aggressive Cl⁻ can “pin on” the Al substrate and result in impressive corrosion rate. According to the above discussion, the increasing fraction of air/water interface per unit area should increase the CA on rough surface, and vice-versa. The superhydrophobic surface can easily trap air within the “valleys” between the “peaks” on the hierarchical interface when immersed in corrosive media, and the liquid forms a convex surface between the interface of the liquid and air for the capillary. Accordingly, the penetration of the aggressive ions (Cl⁻) can be prevented by the “air valleys” between the hierarchically textured structures of superhydrophobic surfaces and render the excellent corrosion resistance.

Finally, we performed Scribe-Grid Test (ASTM D 3359-78) to investigate the adhesion between the film and the Al substrate. Figure 6 shows the photograph of the superhydrophobic Al surface before (a) and after (b) the Scribe-Grid Test. The film showed good adhesion on the Al surface with no delamination or detachment of the film at the edges and within the square lattice observed.

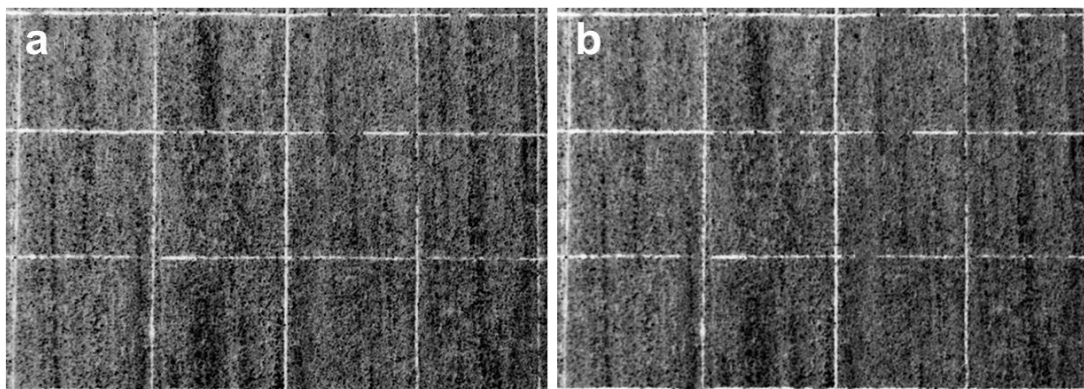


Figure 5: The optical images of the superhydrophobic Al surface before (a) and after (b) the tape test.

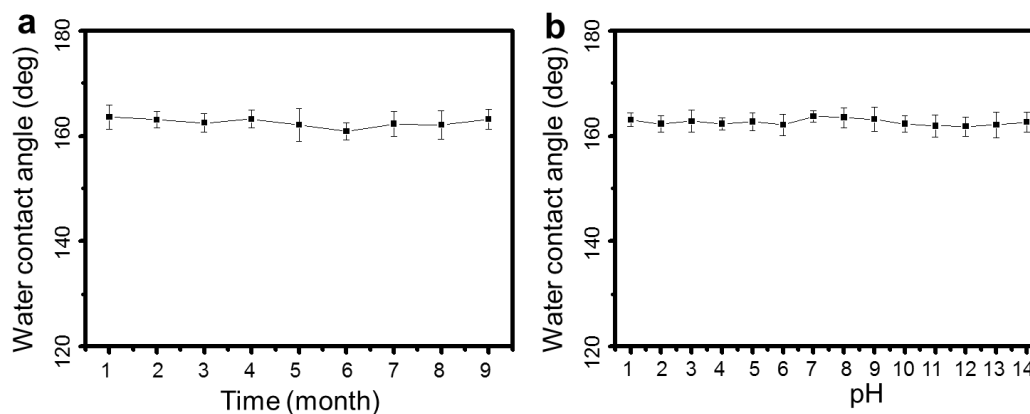


Figure 6: Time (a) and pH (b) dependence of water CAs on the as-prepared superhydrophobic AZ31 surface.

All the plots indicate the averaged values of water CAs measured at five different points on the same sample. The error bars for each plot demonstrate the maximum and minimum water CAs.

4. Conclusions

In summary, superhydrophobic Al surfaces with improved anticorrosion property were successfully constructed by a simple chemical etching process and post-modification with SA. The wettabilities and anticorrosion properties of the obtained Al surfaces were changed with the ratio of DMF to water in modification step due to the combination of low surface free energy SA and surface roughness as well as solvent effect. HCl-etched Al modified with SA in DMF/water mixture solvent with the ratio of DMF to water reaching to 9:1 displayed excellent superhydrophobicity with a CA of 163.4° and a RA of 2.3° and improved anticorrosion property with a corrosion current density of $5.13 \times 10^{-7} \text{ A cm}^{-2}$, which showed promise for “surface engineering” of Al substrates.

References

- [1] A. Kuznetsova, T. D. Burleigh, V. Zhukov, J. Blachere, and J. T. Y. Jr, “Electrochemical Evaluation of a New Type of Corrosion Passivation Layer: Artificially Produced Al_2O_3 Films on Aluminum”, *Langmuir*, vol. 14, no. 9, pp. 2502–2507, 1998.
- [2] D. Chidambaram, C. R. Clayton, and G. P. Halada, “The role of hexafluorozirconate in the formation of chromate conversion coatings on aluminum alloys”, *Electrochimica Acta*, vol.51, no.14, pp. 2862–2871, 2006.
- [3] P. C. Chen, S. J. Hsieh, C. C. Chen, and J. Zou, “A Three Dimensional Enormous Surface Area Aluminum Microneedle Array with Nanoporous Structure”, *Journal of Nanomaterials*, Volume 2013, Article ID 164953, 6 pages.
- [4] R. Cai, M. W. Sun, Z. W. Chen, R. Munoz, C. O’Neill, D. E. Beving, and Y. S. Yan, “Ionothermal Synthesis of Oriented Zeolite AEL Films and Their Application as Corrosion-Resistant Coatings”, *Angewandte Chemie International Edition*, vol. 47, no. 3, pp. 525–528, 2008.
- [5] W. Barthlott, and C. Neinhuis, “Purity of the sacred lotus, or escape from contamination in biological surfaces”, *Planta*, vol. 202, no. 1, pp. 1–8, 1997.

- [6] X. Gao, and L. Jiang, “Water-repellent legs of water striders”, *Nature*, vol. 432, no. 7013, pp. 36–36, 2004.
- [7] Z. X. Xue, S. T. Wang, L. Lin, L. Chen, M. J. Liu, L. Feng, and L. Jiang, “A Novel Superhydrophilic and Underwater Superoleophobic Hydrogel-Coated Mesh for Oil/Water Separation”, *Advanced Materials*, vol. 23, no. 37, pp. 4270–4273, 2011.
- [8] X. Yao, Y. Song, and L. Jiang, “Applications of Bio-Inspired Special Wettable Surfaces”, *Advanced Materials*, vol. 23, no. 6, pp. 719–733, 2011.
- [9] K. S. Liu, and L. Jiang, “Metallic surfaces with special wettability”, *Nanoscale*, vol. 3, no. 3, pp. 825–838, 2011.
- [10] F. Zhang, S. G. Chen, L. H. Dong, Y. H. Lei, T. Liu, and Y. S. Yin, “Preparation of superhydrophobic films on titanium as effective corrosion barriers”, *Applied surface science*, vol. 257, no. 7, pp. 2587–2591, 2011.
- [11] H. Q. Liu, S. Szunerits, M. Pisarek, W. G. Xu, and R. Boukherroub, “Preparation of Superhydrophobic Coatings on Zinc, Silicon, and Steel by a Solution-Immersion Technique”, *ACS Applied Materials & Interfaces*, vol. 1, no. 9, pp. 2086–2091, 2009.
- [12] H. Q. Liu, S. Szunerits, W. G. Xu, and R. Boukherroub, “Preparation of Superhydrophobic Coatings on Zinc as Effective Corrosion Barriers”, *ACS Applied Materials & Interfaces*, vol. 1, no. 6, pp. 1150–1153, 2009.
- [13] Z. X. She, Q. Li, Z. W. Wang, L. Q. Li, F. N. Chen, and J. C. Zhou, “Novel Method for Controllable Fabrication of a Superhydrophobic CuO Surface on AZ91D Magnesium Alloy”, *ACS Applied Materials & Interfaces*, vol. 4, no. 8, pp. 4348–4356, 2012.
- [14] Z. H. Cui, F. Z. Zhang, L. Wang, S. L. Xu, and X. X. Guo, “In Situ Crystallized Zirconium Phenylphosphonate Films with Crystals Vertically to the Substrate and Their Hydrophobic, Dielectric, and Anticorrosion Properties”, *Langmuir*, vol. 26, no. 1, pp. 179–182, 2010.
- [15] F. Z. Zhang, L. L. Zhao, H. Y. Chen, S. L. Xu, D. G. Evans, and X. Duan, “Corrosion Resistance of Superhydrophobic Layered Double Hydroxide Films on Aluminum”, *Angewandte Chemie International Edition*, vol. 47, no. 13, pp. 2466–2469, 2008.
- [16] J. Liang, Y. C. Hu, Y. Q. Wu and H. Chen, “Fabrication and Corrosion Resistance of Superhydrophobic Hydroxide Zinc Carbonate Film on Aluminum Substrates”, *Journal of Nanomaterials*, Vol. 2013, Article ID 139768, 6 pages.
- [17] Y. F. Zhang, H. Wu, X. Q. Yu, and J. Wu, “Facile fabrication of superhydrophobic nanostructures on aluminum foils with controlled condensation and delayed icing effects”, *Applied Surface Science*, Vol. 258, no. 20, pp. 8253–8257, 2012.
- [18] Y. F. Zhang, J. Wu, X. Q. Yu, and H. Wu, “Low-cost one-step fabrication of superhydrophobic surface on Al alloy”, *Applied Surface Science*, Vol. 257, no. 18, pp. 7928–7931, 2011.
- [19] L. Liu, J. Zhao, Y. Zhang, F. Zhao, and Y. Zhang, “Fabrication of superhydrophobic surface by hierarchical growth of lotus-leaf-like boehmite on aluminum foil”, *Journal of Colloid and Interface Science*, Vol. 358, no. 1, pp. 277–283, 2011.
- [20] A. B. D. Cassie, and S. Baxter, “Wettability of porous surfaces”, *Transactions of Faraday Society*, vol. 40, pp. 546–551, 1944.
- [21] T. Ishizaki, and M. Sakamoto, “Facile formation of biomimetic color-tuned superhydrophobic magnesium alloy with corrosion resistance”, *Langmuir*, Vol. 27, no. 6, pp. 2375–2381, 2011.
- [22] N. Q. Wu, L. Fu, M. Su, M. Aslam, K. C. Wong, and V. P. Dravid, “Interaction of fatty acid monolayers with cobalt nanoparticles”, *Nano Letters*, Vol. 4, no. 2, pp. 383–386, 2004.
- [23] S. W. Han, S. W. Joo, T. H. Ha, Y. Kim, and K. Kim, “Adsorption characteristics of anthraquinone-2-carboxylic acid on gold”, *Journal of Physical Chemistry B*, Vol. 104, no. 50, pp. 11987–11995, 2000.